

On the Use of Tomographic derived Reflectivity Profiles for Pol-In-SAR Forest Height Inversion

Roman Guliaev^a, Matteo Pardini^a, Konstantinos P. Papathanassiou^a

^a German Aerospace Center (DLR), Microwave and Radar Institute (HR), Wessling (Germany) – roman.guliaev@dlr.de

Abstract

Model based Pol-InSAR data inversion allows the estimation of forest height using, for example, the RVoG model from single- and multi-baseline Pol-InSAR acquisitions. This conventional approach relies on the approximation of a volumetric reflectivity described by a single parameter, e.g. a constant attenuation coefficient, and assumes in the case of a single baseline that one polarization has almost zero ground response. However, the experimental data imply that for many forest conditions the ground response can be significant in all polarizations, especially at lower frequency bands, e.g. L- and P-band. In addition, the parameterization of RVoG reflectivity by an exponential function might be insufficient. In this paper we propose the parameterization of the forest reflectivity using tomographic reconstructed reflectivity profiles. The separation of ground and volume component in the tomographic data is performed using the (sum of) Kronecker products (SKP) decomposition. The ground contribution is then modeled by a Dirac delta function and the ground to volume ratio is addressed as an unknown parameter together with the forest height. First experimental results demonstrate the improvement in the accuracy and consistency of forest height estimation using the volume separated profiles.

1 Introduction

Polarimetric SAR Interferometry (Pol-InSAR) allows the estimation of forest height by exploiting the correlation between the vertical extent of the 3D reflectivity and interferometric (volume) coherence [1].

A set of interferometric measurements provides a polarization \vec{w} dependent estimate of interferometric coherence $\tilde{\gamma}_{Obs}(\vec{w})$, a complex number which is defined as a multilooked product of the two radar returns (images) $s_1(\vec{w})$ and $s_2(\vec{w})$

$$\tilde{\gamma}_{Obs}(\vec{w}) = \frac{\langle s_1(\vec{w})s_2^*(\vec{w}) \rangle}{\sqrt{\langle s_1(\vec{w})s_1^*(\vec{w}) \rangle \langle s_2(\vec{w})s_2^*(\vec{w}) \rangle}}. \quad (1)$$

The interferometric coherence may contain several independent decorrelation contributions superimposed in a multiplicative way as

$$\tilde{\gamma}_{Obs}(\vec{w}) = \tilde{\gamma}_{Tmp}(\vec{w})\tilde{\gamma}_{Sys}(\vec{w})\tilde{\gamma}_{Vol}(\vec{w}) \quad (2)$$

where $\tilde{\gamma}_{Tmp}(\vec{w})$ is a temporal decorrelation and $\tilde{\gamma}_{Sys}(\vec{w})$ are various system induced decorrelations, such as additive noise decorrelation etc.

Volumetric decorrelation is defined as the Fourier transform of vertical reflectivity $F(z, \vec{w})$ within the reflectivity volume, i.e. from the ground to the top of the forested layer h_v , adjusted to the ground phase ϕ_0

$$\tilde{\gamma}_{Vol}(\kappa_z, \vec{w}) = e^{i\phi_0} \frac{\int_0^{h_v} F(z, \vec{w}) \exp(i\kappa_z z) dz}{\int_0^{h_v} F(z) dz}. \quad (3)$$

The vertical wavenumber κ_z is proportional to the across track baseline, or look angle difference $\Delta\theta$ between the two

acquisitions and inverse proportional to the incidence angle θ_0

$$\kappa_z = m \frac{2\pi}{\lambda} \frac{\Delta\theta}{\sin(\theta_0)} \quad (4)$$

where $m = 2$ for monostatic acquisitions and $m = 1$ for bistatic acquisitions and λ is the radar wavelength.

After normalization, by substituting $z' = z/h_v$, equation (3) rewrites to

$$\tilde{\gamma}_{Vol}(\kappa_z, \vec{w}) = e^{i\phi_0} \frac{\int_0^1 F(z', \vec{w}) e^{i\kappa_z h_v z'} dz'}{\int_0^1 F(z', \vec{w}) dz'}. \quad (5)$$

Thus, if the vertical reflectivity (real) profile is known, forest height can be inverted using the absolute volumetric decorrelation, i.e. using the absolute value on both sides of equation (5) [2] [3].

Polarimetric SAR Tomography (Pol-TomoSAR) allows the reconstruction of the vertical reflectivity $F(z, \vec{w})$ using a large(r) number of conventional or interferometric SAR acquisitions spread over a wide(r) angular range (associated to a certain vertical wavenumber distribution) [4].

Model-free algorithms estimate the 3D reflectivity without making assumptions on the structure of the data or using models to describe them. The algorithms attempt to invert directly the Fourier relationship between data and reflectivity profile. This allows to achieve less constrained results, but makes their interpretation less straightforward. Fourier (FB) [5] and Capon Beamforming (CB) [6] are probably the most used model-free tomographic algorithms. The underlying reflectivity is reconstructed in form of its convolution with the vertical Point Spread Function (PSF) that makes the quality and the vertical resolution of the reconstructed profile strongly dependent on the number and distribution of the available vertical wavenumbers [7].

Accordingly, two parameters characterize the Tomographic reconstruction. The first one is the vertical Rayleigh resolution δ_z that is inversely proportional to the largest vertical wavenumber $k_{z,max} = \max\{k_{zi}\}$ of the available distribution of vertical wavenumbers k_{zi} [4]:

$$\delta_z = \frac{2\pi}{k_{z,max}} \quad (6)$$

The finite sampling in the wavenumber domain causes the appearance of replicas of $F(z, \vec{w})$ in any of its reconstructions. The width of the non-ambiguous tomographic reconstruction height interval, is given (for a uniform distribution of vertical wavenumbers) by [4]:

$$h_{amb} = \frac{2\pi}{k_{z,min}} \quad (7)$$

where $k_{z,min} = \min\{k_{zi}\}$.

Since the tomographic reconstructed profiles represent a convolved profile rather than an actual vertical reflectivity profile, its direct usage for modelling $F(z, \vec{w})$ in the equation of volumetric decorrelation might be undermined.

Limited resolution of the vertical profile might be especially critical at ground level where the real impulse response might have a sharp peak. Depending on the intensity of the ground peak, the resultant interferometric coherence might vary significantly [8].

Therefore, in the next chapter we discuss an approach of modelling the ground response separately from the volumetric reflectivity and rewriting the equation (5) in terms of volume only coherence.

2 Forest height estimation

2.1 Single-baseline forest height and ground to volume ratio estimation model

In the context of the random volume over ground (RVoG) model, the estimation the polarization independent volume coherence $\tilde{\gamma}_{V0}(\kappa_z)$ is attempted under the assumption of a polarisation independent volumetric reflectivity profile approximation, $f_V(z)$ (not necessarily an exponential one). The vertical reflectivity can be then modelled as a two layer (volume only and ground) reflectivity as

$$F(z, \vec{w}) = f_V(z) + m(\vec{w})\delta(z - z_0). \quad (8)$$

where $m(\vec{w})$ is the ground to volume ratio. We propose to use the volume contribution of the tomographic profile $f_{VTomog}(z)$ as an approximation of volume only vertical reflectivity $f_V(z)$. The volume only coherence $\tilde{\gamma}_V(\kappa_z)$ can then be estimated by combining equations (5) and (8)

$$\tilde{\gamma}_{Vol}(\kappa_z, \vec{w}) = \exp(i\varphi_0) \frac{\tilde{\gamma}_V(\kappa_z) + m(\vec{w})}{1 + m(\vec{w})} \quad (9)$$

with

$$\tilde{\gamma}_V(\kappa_z, \vec{w}) = \frac{\int_0^1 f_{VTomog}(z) \exp(i\kappa_z h_V z) dz}{\int_0^1 f_V(z) dz} \quad (10)$$

It is important to note here that, since we do not directly estimate the forest height from equation (10), but rather the unitless product $\kappa_z h_V$, the vertical wavenumber modulates the performance of the forest height estimation, i.e. larger κ_z values give more accurate estimates of lower forest heights while smaller κ_z are required for an accurate estimation of taller forest heights [9] [10].

2.2 Volume/ground reflectivity decomposition

In order to extract the volume only part of the tomographic reconstructed profile, the (sum of) Kronecker products (SKP) decomposition is applied.

Assuming K tomographic tracks, the overall multi-baseline signal $s(\vec{w})$ can be written as the sum of the ground and volume components $s_G(\vec{w})$ and $s_V(\vec{w})$:

$$s(\vec{w}) = s_G(\vec{w}) + s_V(\vec{w}) \quad (11)$$

Supposing the ground and volume components statistically independent, the covariance matrix $R(\vec{w})$ of $s(\vec{w})$ is given by [11] [12] [13]:

$$R(\vec{w}) = m_G(\vec{w})\Gamma_G + m_V(\vec{w})\Gamma_V \quad (12)$$

where $m_G(\vec{w})$ and $m_V(\vec{w})$ are the ground and volume backscattering powers, and Γ_G and Γ_V contain the associated interferometric coherences. If N_p polarisations are available, the related data vectors can be stacked one on top of the other in a single $N_p K$ -dimensional data vector y_p . The covariance matrix of y_p is then [9]:

$$R_p = C_G \otimes \Gamma_G + C_V \otimes \Gamma_V \quad (13)$$

where “ \otimes ” denotes the Kronecker matrix product and C_G and C_V are the polarimetric covariance matrices of the ground and volume, respectively. Model (9) is intrinsically ambiguous: an ensemble of Γ_G , Γ_V , C_G and C_V can be combined to provide the same R_p . A least squares optimization can only provide candidate estimates of Γ_G and Γ_V [9]:

$$\Gamma_G = aR_1 + (1-a)R_2, \quad \Gamma_V = bR_1 + (1-b)R_2 \quad (14)$$

where R_1 and R_2 are two $(K \times K)$ -dimensional matrices obtained from the singular value decomposition of a permuted version of R_p [9]. The scalars a and b vary in intervals that make the four matrices positive semi-definite and define the ambiguity of the reconstruction.

2.3 Application on experimental data

The Pol-TomoSAR data were collected in Lopé National Park in Gabon during the AfriSAR campaign by the DLR's F-SAR airborne platform on Feb. 10, 2016 [14].

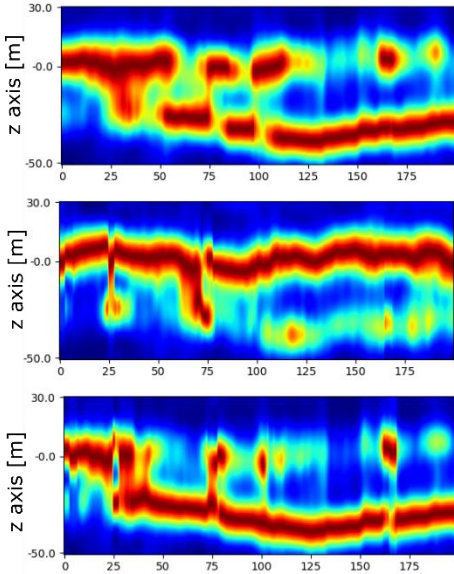


Fig. 1 P-band tomographic FB profiles in Lopé forest. The z-direction corresponds to the vertical axis with $z=0$ corresponding to the reference DEM (TanDEM-X DEM) position. From top to bottom: HH-pol FB profile, polarization independent SKP desomposed volume only and ground profiles.

Fig. 1 illustrates the FB reconstructed tomographic profiles using a tomographic stack of eleven baselines, with an almost uniform κ_z distribution resulting in the Rayleigh resolution of around 15 m. The Lopé tropical forest is characterised by dense vegetation and therefore projects high intensity reflection from the top forest layer, even at P-band. The SKP-decomposed profiles are shown in the middle and bottom of Fig. 1.

The ground separated profile is used to estimate ground phase by searching the position of the lowest peak in the tomogram [15]

The volume only separated profile is used as an approximation of the vertical reflectivity shape in equation (10). For the profile normalization the upper boundary was determined from volume only tomographic profile by searching the position of the highest relevant peak in the profile.

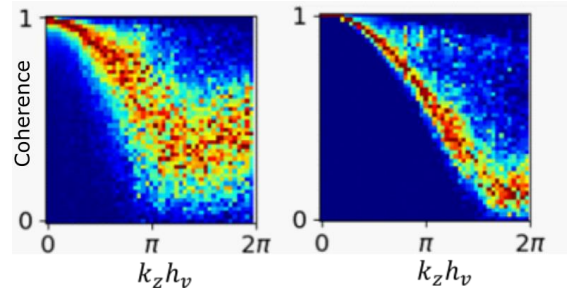


Fig. 2.: Interferometric coherence for different values of parameter $\kappa_z h$. Left plot: interferometric coherence from interferometric measurements, right plot: interferometric coherence modeled using individual tomographic profiles.

Once the ground position and the normalized profile are determined for each sample within the region of interest, the forest height and ground to volume ratio estimation is performed using the equation (9). The performance plots are provided in Fig. 3, with an implication that using volume separated profiles result in a more accurate forest height estimation.

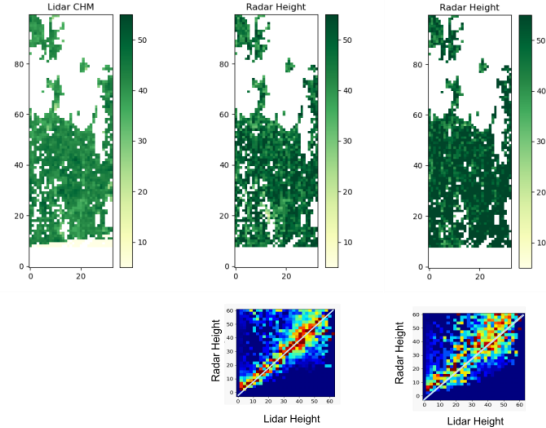


Fig. 3 Forest height inversion using TomoSAR FB profiles and Volume separated TomoSAR FB profiles in Lopé forest at HH-pol $\kappa_z \approx 0.07 - 0.11$. Forest-non-forest mask was applied. Top row from left to right: LiDAR RH100 reference CHM map, radar estimated height using volume separated TomoSAR FB profiles and radar estimated height using TomoSAR FB profile. Bottom row: validation histograms.

Fig. 2 demonstrates why using the tomographic reconstructed profiles directly does not always lead to the accurate forest height estimation. It provides the interferometric coherence value distribution at different values of unitless parameter $k_z h_v$, i.e. various vertical wavenumbers and forest heights (taken from Land, Vegetation, and Ice Sensor (LVIS) lidar RH100 reference [16]). The inconsistency between the experimental interferometric coherence and the interferometric coherence modelled from the tomographic profiles becomes evident by comparing the two distributions in Fig. 2.

3 Outlook

The proposed forest height estimation approach can be extended to the case multibaseline forest height estimation. In this case one would also be able to account for temporal decorrelation effects and/or change in the structure of volumetric reflectivity profile.

In the full paper we will address the performance of the forest height estimation at different baselines and polarizations. Forest height inversion within certain range should ideally be independent of κ_z and polarization, though the inverted ground to volume ratio can be different for different polarizations. The proposed forest height estimation method has a high relevance, especially in the light of upcoming space-borne SAR missions (as ESA's BIOMASS or ROSE-L Plus) able to acquire polarimetric, interferometric and tomographic data.

4 Bibliography

- [1] S. Cloude and K. Papathanassiou, "Three-stage inversion process for polarimetric SAR interferometry," *IEEE Proc. – Radar Sonar Navig.*, vol. 150, no. (3), pp. 125-134, 2003.
- [2] R. Guliaev, V. Cazcarra-Bes, M. Pardini and K. Papathanassiou, "Forest Height Estimation by Means of TanDEM-X InSAR and Waveform Lidar Data.," *IEEE Journal of Selected Topics in Applied Earth Observations and Remote Sensing*, vol. 14, pp. 3084-3094, 2021.
- [3] C. Hao, S. Cloude and J. White, "Using GEDI Waveforms for Improved TanDEM-X Forest Height Mapping: A Combined SINC+ Legendre Approach," *Remote Sensing*, vol. 13, no. 15, p. 2882, 2021.
- [4] A. Reigber and A. Moreira, "First demonstration of air-borne SAR tomography using multibaseline L-band data," *IEEE Trans. Geosci. Remote Sens.*, vol. 38, no. 5, pp. 2142-2152, Sept. 2000.
- [5] P. Stoica and R. Moses, *Spectral analysis of signals*, 2005.
- [6] F. Lombardini and A. Reigber, "Adaptive spectral estimation for multibaseline SAR tomography with airborne L-band data," *IEEE International Geoscience and Remote Sensing Symposium. Proceedings (IEEE Cat. No. 03CH37477)*, vol. 3, 2003..
- [7] V. Cazcarra Bes, M. Pardini, M. Tello and M. Papathanassiou, "Comparison of Tomographic SAR Reflectivity Reconstruction Algorithms for Forest Applications at L-band," *IEEE Trans. Geosci. Remote Sens.*.
- [8] S. Cloude, *Polarisation: applications in remote sensing*, Oxford: OUP, 2009.
- [9] Z. Liao, B. He, A. I. van Dijk, X. Bai and X. Quan, "The impacts of spatial baseline on forest canopy height model and digital terrain model retrieval using P-band PolInSAR data," *Remote Sensing of Environment*, vol. 210, pp. 403-421, 2018.
- [10] F. Kugler, S.-K. Lee and K. Papathanassiou, "Forest Height Estimation by means of Pol-InSAR Data Inversion: The Role of the Vertical Wavenumber," *IEEE Trans. Geosci. Remote Sens.*, vol. 53, no. 10, 2015.
- [11] M. Pardini and K. Papathanassiou, "'On the estimation of ground and volume polarimetric covariances in forest scenarios with SAR tomography.,"" *IEEE Geoscience and Remote Sensing Letters*, vol. 14, no. 10, pp. 1860-1864., 2017.
- [12] S. Tebaldini, "Algebraic synthesis of forest scenarios from multibaseline PolInSAR data," *IEEE Trans. Geosci. Remote Sens.*, vol. 47, no. 12, p. 4132-4142, 2009.
- [13] S. Tebaldini, "Single and multipolarimetric SAR tomography of forested areas: A parametric approach," *IEEE Trans. Geosci. Remote Sens.*, vol. 48, no. 5, p. 2375-2387, 2010.
- [14] I. Hajnsek, M. Pardini, et al., "Technical assistance for the development of airborne SAR and geophysical measurements during the AfriSAR campaign, Final technical report".
- [15] M. Pardini, M. Tello, V. Cazcarra-Bes, K. Papathanassiou and I. Hajnsek, "L-and P-band 3-D SAR reflectivity profiles versus lidar waveforms: The AfriSAR case.," *IEEE Journal of Selected Topics in Applied Earth Observations and Remote Sensing*, vol. 1, 2018.
- [16] J. Blair and M. Hofton, "AfriSAR LVIS L2 Geolocated Surface Elevation Product, Version 1. Boulder, Colorado USA. NASA National Snow and Ice Data Center Distributed Active Archive Center," [Online]. [Accessed 2018].